

## NOVA-INDUCED MASS TRANSFER VARIATIONS

U. KOLB

Department of Physics and Astronomy, The Open University,  
 Walton Hall, Milton Keynes MK7 6AA, UK

S. RAPPAPORT

Department of Physics and Center for Space Research  
 Massachusetts Institute of Technology, Cambridge, MA 02139

K. SCHENKER

Department of Physics & Astronomy, University of Leicester,  
 University Road, Leicester LE1 7RH, UK

AND

S. HOWELL

Astrophysics Group, Planetary Science Institute  
 620 N. 6th Avenue, Tucson, AZ 85705

*Accepted for publication in ApJ (August 2001)*

### ABSTRACT

We investigate variations of the mass transfer rate in cataclysmic variables (CVs) that are induced by nova outbursts. The ejection of nova shells leads to a spread of transfer rates in systems with similar orbital period. The effect is maximal if the specific angular momentum in the shell is the same as the specific orbital angular momentum of the white dwarf. We show analytically that in this case the nova-induced widening of the mass transfer rate distribution can be significant if the system, in the absence of nova outbursts, is close to mass transfer instability (i.e., within a factor of  $\sim 1.5$  of the critical mass ratio). Hence the effect is negligible below the period gap and for systems with high-mass white dwarfs. At orbital periods between about 3 and 6 hrs the width of the mass transfer rate distribution exceeds an order of magnitude if the mass accreted on the white dwarf prior to the runaway is larger than a few  $10^{-4}M_{\odot}$ . At a given orbital period in this range, systems with the highest transfer rate should on average have the largest ratio of donor to white dwarf mass. We show results of population synthesis models which confirm and augment the analytic results.

*Subject headings:* novae, cataclysmic variables – stars: binaries: close – stars: evolution – stars: mass loss – stars: low mass

### 1. INTRODUCTION

A long-standing problem in the theory of cataclysmic variable (CV) evolution is the large scatter of observationally deduced mass transfer rates for systems with similar orbital periods (Patterson 1984, Warner 1987, Warner 1995). This appears to be in conflict with the well founded assumption that mass transfer in CVs is driven by orbital angular momentum losses such as gravitational radiation and magnetic braking (see, e.g., Rappaport, Joss, & Webbink 1982 (RJW), Rappaport, Verbunt, & Joss 1983 (RVJ), Hameury et al. 1988; for a review see, e.g., King 1988).

Binary evolution calculations have shown that CVs that form with different initial secondary masses converge rather quickly to an essentially unique track in, e.g., the orbital period – mass transfer rate ( $P_{\text{orb}} - \dot{M}$ ) space (e.g., RVJ, Kolb & Ritter 1992). This track convergence arises as the angular momentum loss rate, and hence the mass transfer rate itself, depend on the current system parameters only. Low-mass main-sequence stars that are subject to mass loss rapidly settle at a new equilibrium radius  $R_2$  (Stehle et al. 1996) which in turn is a function of the mass loss timescale. Therefore the orbital period  $P_{\text{orb}} \propto R_2^{3/2}$  of systems at the equilibrium radius is set by the mass

transfer rate.

The track convergence implies that any variation of  $\dot{M}$  at a fixed  $P_{\text{orb}}$  should largely reflect the dependence of the angular momentum loss rate  $\dot{J}$  on the white dwarf mass  $M_1$ . Since  $-\dot{M}_2/M_2 \propto \dot{J}/J$ , cf. eq (11) below, and  $\dot{J}$  has no explicit dependence on  $M_1$  for mechanisms like magnetic braking which are rooted in the secondary star, the expected dependence on  $M_1$  at a fixed period is  $\propto (M_1 + M_2)^{1/3}/M_1$ . This is too weak in view of the observed scatter of at least an order of magnitude.

Classical nova outbursts represent an obvious mechanism that could cause deviations of the transfer rate from the secular mean value set by the angular momentum loss rate. All CVs are expected to experience some form of nuclear burning of the accreted hydrogen-rich material on the surface of the white dwarf (WD). In most cases this should be non-steady and lead to systemic mass loss, e.g. in the form of a classical nova outburst. Specifically, in the following we assume that the burning is episodic and always accompanied by the ejection of the layers that are affected by the burning, i.e., the nova shell. The ejection occurs on a very short timescale ( $\lesssim$  months) and effectively leads to an instantaneous change of the orbital separation. The magnitude and sign of the change are determined by

the amount of angular momentum the shell removes from the orbit. In most cases the orbital separation increases, with a resulting drop of the mass transfer rate, as the Roche lobe is moved suddenly outward by a few atmospheric pressure scale heights from the photosphere. The effect is largest if the angular momentum per unit mass in the nova shell is minimal. For an axi-symmetric ejection this minimum is just the specific orbital angular momentum of the white dwarf. We refer to such hydrodynamic ejections as *ballistic*, irrespective of the physical nature of the ejection mechanism (e.g., nova explosions, optically thick winds from the white dwarf, and so forth).

If there is additional angular momentum transfer from the binary orbit to the nova envelope due to dynamical friction of the secondary orbiting inside this envelope the increase of the orbital separation upon envelope ejection is smaller than in the ballistic case. Very strong frictional transfer would even lead to a decrease of the separation.

The approach taken by MacDonald (1986) to model dynamical friction in the nova envelope gave an extremely efficient extraction of angular momentum from the orbit. The concomitant mean orbital evolution was greatly accelerated and resulted in both very large mean mass transfer rates ( $\gtrsim 10^{-7} M_{\odot} \text{yr}^{-1}$ ), and a greater spread of the mean mass transfer rate at a given orbital period than in the absence of nova outbursts. Such a variation of the *mean* transfer destroys the coherence of evolutionary tracks we noted above, and is therefore in conflict with the standard model for the CV orbital period gap (see e.g. Kolb 1996). MacDonald did not consider the effect of individual outbursts on the mass transfer rate distribution.

In contrast, Schenker, Kolb, & Ritter (1998), following Livio, Govarie, & Ritter (1991) to model dynamical friction, found a much weaker angular momentum transfer by dynamical friction. Schenker et al. largely dismissed the effect of nova outbursts on the mass transfer rate distribution as unimportant, for ballistic ejections as well as for cases with plausible friction. Note that for the remainder of this paper we use the terms “mass transfer rate distribution” and “mass transfer rate spectrum” interchangeably. More precisely, they both describe the distribution in values of  $\dot{M}$  at a given orbital period, for either the evolution of a single CV or an ensemble of CVs, as a function of orbital period.

A closely related issue is the notion that CVs “hibernate” after nova outbursts, i.e., there has been the suggestion that post-novae are very faint, for a time comparable to the nova recurrence time (Shara et al. 1986; Prialnik & Shara 1987, Livio & Shara 1987). The hibernation idea was motivated by space density issues, the need for smaller mass transfer rates to obtain violent nuclear runaways in theoretical nucleosynthesis models, and by observations suggesting that the remnant systems of historical novae are faint.

In this work we reconsider the maximum possible variation of the mass transfer rate about the secular mean rate due to the ballistic ejection of nova shells. In Section 2 we review the methods by which the mass transfer rates in CVs are deduced. We conclude that while some of the spread in the  $\dot{M}$ 's is due to the uncertainties in determining the transfer rates, much of the spread is due to a real variation among different systems. In Section 3

we develop a simple analytical description for the time-dependent behavior of  $\dot{M}$  between nova outbursts, as well for the probability densities for  $\dot{M}$  at a given orbital period (with technical details deferred to the Appendix). In this same section we apply the analytic model to find the previously ignored optimum system parameter combination that maximizes the spread of mass transfer rates at a given orbital period in an observed sample of CVs. In Section 4 we use this prescription in population synthesis models to show the overall effect on a theoretical CV population with standard assumptions about their formation and evolution. A significant fraction of the CV population lies in the optimum parameter range found in Section 3. Finally in Section 5 we draw conclusions concerning the likely effects of nova explosions on the spread in values of  $\dot{M}$  observed in CVs.

## 2. DETERMINATION OF $\dot{m}$ IN CVS

Observational determinations of the mass accretion rate in cataclysmic variables show a large spread of order 10 up to 100 in  $\dot{M}$  at a given orbital period, being most pronounced in the period range of 3 to 6 hr (see Fig. 9.8 in Warner 1995). Before presenting our model which may partially account for this substantial spread we briefly review the observational methods used to determine  $\dot{M}$  and examine what “spread” may be introduced simply by uncertainties in the measurements or the assumptions that go into the analysis and interpretation of the data.

Smak (1989) computed  $\dot{M} - M_V$  relationships for standard thin accretion disks using the usual multi-temperature black-body approximations. These relations are still often used for determinations of  $\dot{M}$  (see, e.g., Robinson et al. 1999). Smak (1994) later added a finite disk thickness to account for a bright disk rim and a less oblique view of the far side of the disk. He found that  $M_V$  increased by only 0.5 magnitudes in most cases for moderate to low binary inclinations  $i$ , while at large values of  $i$  and/or high transfer rates, changes in  $M_V$  of up to 2.5 magnitudes are possible. Smak's results show that for high mass accretion rates ( $10^{-8} - 10^{-9} M_{\odot} \text{yr}^{-1}$ ) a perfectly known value of  $M_V$  corresponds to an uncertainty in accretion rate of a factor of  $\sim 2 - 10$  at a given orbital period.

To make use of the  $\dot{M} - M_V$  relations, the value of  $M_V$  for the disk is needed. Observational determinations of  $M_V$  are usually based upon the belief that in the optical V band, the flux received is almost entirely from the accretion disk. For CVs with orbital periods in the range of 3 – 6 hr, this is a fairly safe assumption. Thus, using some method of distance determination, and accounting for the binary inclination (see Warner 1995 for the convention used to convert the observed value into a common definition of  $M_V$ ), one can then estimate  $\dot{M}$ . To the uncertainties inherent in the  $\dot{M} - M_V$  relationships one should also add the rather substantial uncertainties in the distance determinations which are used to find  $M_V$ .

An independent method of checking whether these  $\dot{M}$  estimates are reasonable, which is not based on the determination of  $M_V$ , is to utilize X-ray observations and simple accretion disk/boundary layer theory. Here the basic assumption is that some fraction of the accretion luminosity,

$GM_1\dot{M}/R_1$ , will emerge in X-radiation. Thus, if the mass  $M_1$  and radius  $R_1$  of the white dwarf are known to some degree from observation or by assumption, measurements of  $L_X$  can be used to estimate  $\dot{M}$  (see Frank et al. 1992). Patterson and Raymond (1985a) provided a comparison of observed  $L_X$  with a suitable observed mean of  $\dot{M}$  as a function of orbital period, derived from  $\dot{M}$  estimates by other methods (e.g. Patterson 1984), and found the following: Using an optically thick boundary layer model the two estimates of  $\dot{M}$  agreed to within a factor of 5 at low  $\dot{M}$  ( $10^{-10.5} M_\odot \text{ yr}^{-1}$ ) and 10 at high  $\dot{M}$  ( $10^{-8.5} M_\odot \text{ yr}^{-1}$ ).

Another powerful method to estimate  $\dot{M}$  is photometric eclipse mapping. This uses the standard relation  $T^4(R) \simeq 3GM_1\dot{M}/8\pi r^3$  between disk temperature  $T$  and disk radius  $r$  to allow an estimate of  $\dot{M}$  (Horne 1985). If multicolor light curves are available, and the effect of reddening can be estimated, this method is independent of distance determinations. Smak (1994) showed that for  $\dot{M} \gtrsim 10^{-8} M_\odot \text{ yr}^{-1}$  (orbital periods of greater than  $\sim 5$  hr), this technique can yield spurious results. However, for typical systems in the 3–6 hr range, the agreement between the observed and theoretically expected  $T^4(R)$  profiles is generally good, with deviations being a factor of 10 or less. Baptista (2000) reviews the current level of knowledge in this area.

Yet another method, using equivalent widths of disk emission lines, is based on apparent relationships between the strength of the disk emission lines and  $M_V$  from the accretion disk. For example, Patterson (1984) used the equivalent width of H $\beta$  to present a set of accretion disk  $\dot{M}$  values. Smak (1989), however, noted that Patterson used a mixture of thin and thick accretion disks at various binary inclinations and his assumed  $\dot{M}$  values were based on an  $\dot{M} - M_V$  relation by Tytenda (1981) which, in turn, used an unrealistically large accretion disk. Thus, the determined  $\dot{M}$  values are likely to be underestimated in general by factors of 2–6. Using the strength of He II emission, an assumed white dwarf mass of  $0.7 M_\odot$ , and a 3 Å equivalent width for the line, Patterson and Raymond (1985b) found agreement between the values of  $\dot{M}$  predicted by their method, and the values of  $\dot{M}$  estimated by other methods to within factors of 5–10 over a broad range of  $\dot{M}$  for a number of CVs.

We find that, in general, the observational determinations of  $\dot{M}$  have typical associated uncertainties of factors of  $\sim 3 - 5$  and in some cases up to a factor of  $\sim 10$ . From this information we would conclude that the observed spread in the  $\dot{M}$  distribution, which is found to approach factors of 100, especially for the 3–6 hr orbital period range, is in large part a real effect.

In the final analysis, however, perhaps the best evidence in favor of a wide spread in the values of  $\dot{M}$  at a given  $P_{\text{orb}}$ , is the coexistence of dwarf novae and nova-like variables at the same orbital period. The widely accepted explanation for dwarf nova eruptions is provided by thermal ionization instabilities in their accretion disks (Meyer & Meyer-Hofmeister 1981; Cannizzo, Shafter, & Wheeler 1988; for a review see e.g. Frank et al. 1992) which, in turn, require smaller values of  $\dot{M}$  than are inferred for nova-like variables which exhibit no such disk instabilities.

### 3. ANALYTIC MODEL

In this section we develop an analytic model for the mass transfer rate spectrum that is induced by the ballistic ejection of nova shells. For convenience we defer a portion of the derivation to the Appendix. After introducing standard definitions describing mass transfer via Roche-lobe overflow we simply present the main resulting expressions and focus on their discussion.

#### 3.1. Stationary and nonstationary mass transfer

For simplicity of notation, let  $\dot{M}$  be the magnitude of the mass transfer rate, i.e.,

$$\dot{M} = -\dot{M}_2 > 0, \quad (1)$$

where  $M_2$  is the mass of the Roche-lobe filling secondary. In general, the transfer rate is a sensitive function of the difference between the stellar (photospheric) radius  $R$  and the Roche lobe radius  $R_L$  of the secondary. In the case of CVs a good approximation is

$$\dot{M} = \dot{M}_{ph} \exp \left\{ \frac{R - R_L}{H} \right\}. \quad (2)$$

Here  $H$  is the photospheric pressure scale height of the secondary star, and  $\dot{M}_{ph}$  is the mass transfer rate when the Roche lobe is situated at the photospheric radius (see, e.g., Ritter 1988, Kolb & Ritter 1990). Typical values of  $\dot{M}_{ph}$  for low-mass main-sequence stars are expected to be  $\sim 10^{-8} M_\odot \text{ yr}^{-1}$ .

Over intervals that are short compared to the mass loss time scale  $t_M = M_2/\dot{M}$ , the time derivative of the transfer rate (2) is

$$\frac{d\dot{M}}{dt} \simeq \dot{M} \frac{R}{H} \left\{ \frac{\dot{R}}{R} - \frac{\dot{R}_L}{R_L} \right\} \quad (3)$$

if  $\dot{M}_{ph}$  and  $H$  are constant and  $R - R_L \ll R$ .

To make use of (3) we introduce the standard decomposition of radius derivatives into mass transfer-dependent and independent terms (e.g. RVJ, Webbink 1985, Ritter 1996),

$$\frac{\dot{R}}{R} = \zeta \frac{\dot{M}_2}{M_2} + \left( \frac{\partial \ln R}{\partial t} \right)_{\text{th}} \quad (4)$$

$$\frac{\dot{R}_L}{R_L} = \zeta_L \frac{\dot{M}_2}{M_2} + 2 \left( \frac{\dot{J}}{J} \right)_{\text{sys}}. \quad (5)$$

Here the stellar mass-radius index  $\zeta$  describes the adiabatic response of the donor star to mass loss, while  $(\partial \ln R / \partial t)_{\text{th}}$  denotes the relative radius change due to thermal relaxation. (We neglect any changes of the radius due to nuclear evolution).  $\zeta_L$  is the Roche-lobe index and encompasses changes of the Roche lobe due to mass transfer and mass loss, and  $\dot{J}_{\text{sys}}$  are “systemic” orbital angular momentum losses unrelated to mass loss (e.g., due to gravitational radiation and magnetic braking).  $J$  is the total orbital angular momentum.

With (4) and (5) equation (3) can be written as

$$\frac{d\dot{M}}{dt} = \frac{1}{\epsilon} \frac{\dot{M}}{M_2} \left\{ \frac{M_2}{t_{\text{ev}}} - D\dot{M} \right\}, \quad (6)$$

where we have introduced the relative thickness of the photosphere of the donor star,

$$\epsilon = H/R, \quad (7)$$

(for CVs,  $\epsilon \simeq 10^{-4}$ ), the stability denominator

$$D = \zeta - \zeta_L, \quad (8)$$

usually of order unity, and the evolutionary timescale  $t_{\text{ev}}$ ,

$$\frac{1}{t_{\text{ev}}} = \left( \frac{\partial \ln R}{\partial t} \right)_{\text{th}} - 2 \left( \frac{j}{J} \right)_{\text{sys}}. \quad (9)$$

From (3) we see that mass transfer is stationary ( $d\dot{M}/dt = 0$ ) if

$$\frac{\dot{R}}{R} = \frac{\dot{R}_L}{R_L}, \quad (10)$$

and (6) shows that in stationarity the mass transfer rate is

$$\dot{M}_s = \frac{M_2/t_{\text{ev}}}{D}. \quad (11)$$

Hence the transfer rate is of order  $M_2/t_{\text{ev}}$ , unless the system is close to instability where  $D$  is small (see e.g. RJW, RVJ, King & Kolb 1995 for a discussion of mass transfer instability).

### 3.2. Nova outbursts

To apply this formalism to CVs that experience repeated nova outbursts we consider both the actual evolution between outbursts, and a mean evolution.

We assume that the evolution between outbursts is conservative, i.e., none of the transferred mass is lost from the system.

The outburst itself is treated as an instantaneous ejection of the nova shell with mass  $\Delta M_{\text{ej}}$ . If this is related to the accreted mass  $\Delta M_{\text{ign}}$  needed to trigger the thermonuclear runaway as

$$\Delta M_{\text{ej}} = \gamma \Delta M_{\text{ign}} = -\gamma \Delta M_2 > 0, \quad (12)$$

( $\gamma > 0$ ), then the ratio of maximum to minimum values of  $\dot{M}$  during an outburst cycle is

$$\frac{\dot{M}_f}{\dot{M}_0} = \exp \left( \frac{1}{\epsilon} \gamma \frac{4}{3} \frac{\Delta M_{\text{ign}}}{M_b} \right) = \exp \left( \frac{1}{\epsilon} \frac{4}{3} \frac{\Delta M_{\text{ej}}}{M_b} \right), \quad (13)$$

where  $\dot{M}_f$  and  $\dot{M}_0$  are the values of  $\dot{M}$  just before and just after a nova explosion, respectively, and  $M_b$  is the total mass of the binary. Equation (13) assumes that the ejected mass carries away the mean specific orbital angular momentum of the white dwarf. In this case the Roche lobe of the secondary always increases as a result of a nova outburst, leading to a sudden drop of the mass transfer rate.

We assume that the nova outburst recurrence time  $t_{\text{rec}}$  is sufficiently short so that the donor mass  $M_2$ , the relative thickness  $\epsilon = H/R$  of the photosphere and the evolutionary timescale  $t_{\text{ev}}$  can be considered as constant between outbursts. Then, by direct integration of eq. (6), the transfer rate between  $t = 0$ , the time immediately after the outburst, and  $t = t_{\text{rec}}$ , the time immediately before the next outburst, is

$$\dot{M}(t) = \frac{\dot{M}_c}{1 + (\dot{M}_c/\dot{M}_0 - 1) \exp(-t/\epsilon t_{\text{ev}})}. \quad (14)$$

(see, e.g., Schenker et al. 1998). Here  $\dot{M}_c$  is the stationary mass transfer rate the system would adopt (for conservative transfer) in the absence of nova outbursts, except when it is dynamically unstable. A strict definition of  $\dot{M}_c$  is given in the Appendix, see equation (A12).

### 3.3. Mass transfer rate spectrum

Consider now an ensemble of CVs with similar component masses ( $M_1, M_2$ ) and mean mass transfer rate  $\dot{M}_m$  at orbital period  $P$ . The mean transfer rate is defined by

$$\dot{M}_m = \frac{1}{t_{\text{rec}}} \int_0^{t_{\text{rec}}} \dot{M}(t) dt \quad (15)$$

and corresponds to the “fiducial” mean evolution where the sequence of discontinuous mass ejections is replaced by a continuous, isotropic wind, such that  $\dot{M}_{\text{wind}} = \Delta M_{\text{ej}}/t_{\text{rec}}$ .

Then the actual (instantaneous) mass transfer rates in the ensemble are between  $\dot{M}_0$  and  $\dot{M}_f = \dot{M}(t_{\text{rec}})$ . The probability density distribution  $n(\dot{M})$  in  $\dot{M}$  space is proportional to  $1/\dot{M}$ , so that the normalized mass transfer rate spectrum reads

$$n(\dot{M}) = \frac{1}{t_{\text{rec}}} \frac{dt}{d\dot{M}}(\dot{M}) \quad (16)$$

( $\int n(\dot{M}) d\dot{M} = 1$ ). With  $dt/d\dot{M} = 1/(d\dot{M}/dt)$  we obtain by manipulating equation (6):

$$\frac{dt}{d\dot{M}} = \epsilon t_{\text{ev}} \frac{\dot{M}_c}{(\dot{M}_c - \dot{M}) \dot{M}}. \quad (17)$$

As can be seen from (13) the full ratio of mass transfer rates exceeds an order of magnitude if the ejected mass is larger than about  $10^{-4} M_{\odot}$ . Yet, in many cases, the systems still spend most of their time close to the secular mean  $\dot{M}_m$ , even if the amplitude is large. The corresponding mass transfer rate spectrum  $\tilde{n}(\log \dot{M}) \propto \dot{M} n(\dot{M})$  has a narrow spike at large transfer rates, and a long tail with low probability density toward small  $\dot{M}$ . An illustrative example of  $\dot{M}$  vs. time during the interval between nova events is shown in the upper panel of Fig. 1. The lower panel in the same figure shows the corresponding probability density in  $\dot{M}$ . The cases studied by Schenker et al. (1998) had an even narrower distribution than the example shown in Fig. 1.

To judge the effective “width” of the distribution in  $\dot{M}$ -space we consider the half width  $w$  to be the following ratio:

$$w \equiv \frac{\dot{M}_f}{\dot{M}_{1/2}}, \quad (18)$$

where  $\dot{M}_{1/2} = \dot{M}(t_{\text{rec}}/2)$  is the median of the mass transfer rate distribution (16), i.e.

$$\int_{\dot{M}_0}^{\dot{M}_{1/2}} n(\dot{M}) d\dot{M} = \int_{\dot{M}_{1/2}}^{\dot{M}_f} n(\dot{M}) d\dot{M}. \quad (19)$$

As a working criterion, we adopt the condition  $w > 10$  to signal a “wide distribution”. If we define a “stability” ratio

$$\alpha = \frac{2D_c}{D_m} \quad (20)$$

and a mass accumulation factor

$$x = \exp \left( \frac{D_m}{2\epsilon} \frac{\Delta M_{\text{ign}}}{M_2} \right) \quad (21)$$

( $x \geq 1$ ), then equations (14) and (18) and the above definitions can be combined to yield the following expression for  $w$ :

$$w(x) = \frac{x(1 + x^{1-\alpha})}{1 + x}. \quad (22)$$

The stability denominators  $D_c$  and  $D_m$  are given by (8) and refer to the conservative evolution between outbursts and the time-averaged evolution, respectively. The stellar index is the same for both  $D_c$  and  $D_m$ , while the appropriate Roche lobe indices are given in the Appendix.

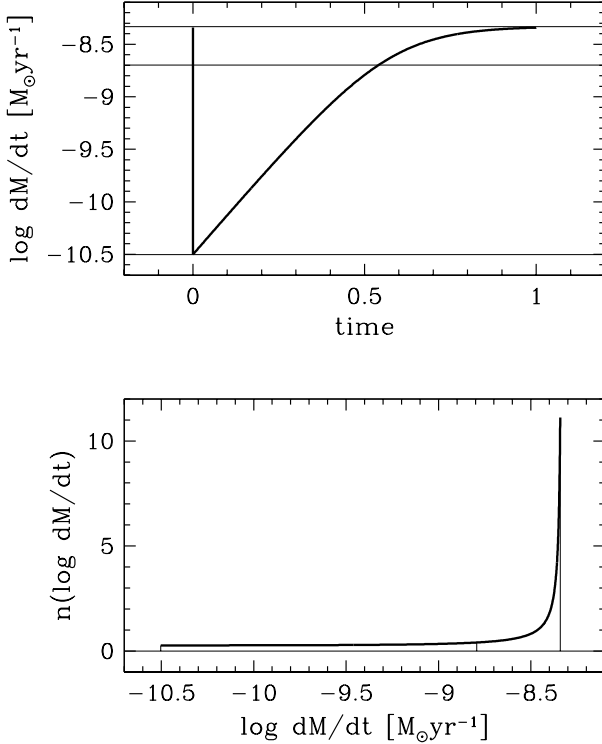


FIG. 1.— *Upper panel*: Typical evolution of the mass transfer rate  $\dot{M}$  between nova outbursts (here for  $M_2 = 0.3M_\odot$ ,  $M_1 = 0.6M_\odot$ ,  $\Delta M_{\text{ign}} = 3 \times 10^{-5}M_\odot$ ). The time is in units of the recurrence time. The upper solid line is the asymptotic value  $\dot{M}_c$ , the lower solid line the time-average  $\dot{M}_m = 2 \times 10^{-9}M_\odot \text{yr}^{-1}$ . *Lower panel*: The corresponding probability density distribution  $n(\log \dot{M})$ .

As  $\zeta$  is essentially a function of stellar mass, and  $\zeta_L$  is a function of the mass ratio  $q$ ,

$$q = \frac{M_2}{M_1}, \quad (23)$$

only, the stability factor  $\alpha$  is fixed for a given system. In contrast, the mass accumulation factor  $x$  depends on the ignition mass. Observational estimates of nova ejecta masses, though subject to large uncertainties, tend to give much larger values than results of detailed model calculations of the thermonuclear runaway on the surface of hydrogen-accreting white dwarfs (see, e.g., Starrfield 1999 and references therein). Hence we examine  $w$  as a function of  $x$  in order to provide possibly new insight into nova ejecta masses based on the spread in CV mass transfer rates.

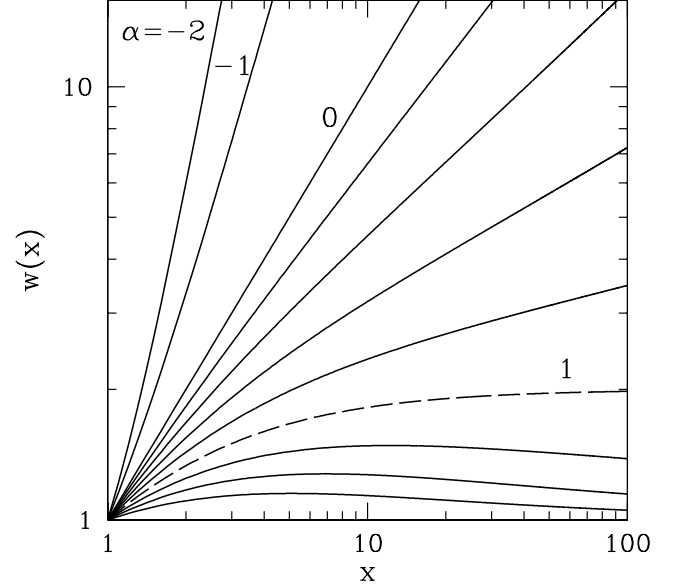


FIG. 2.— Half width  $w(x)$  as a function of mass accumulation factor  $x$ , for different stability ratios  $\alpha$  (as labelled). The dashed curve is the limiting case  $\alpha = 1$ . The  $\alpha$  increment between the curves is 0.2 if  $\alpha > 0$ .

The shape of  $w(x)$  depends on the value of the parameter  $\alpha$  which describes the stability of mass transfer in the system. We require that CVs are dynamically stable with respect to the mean evolution, i.e.,  $D_m > 0$ . As the nova shell carries the mean specific orbital angular momentum of the WD we also have  $D_c < D_m$ , hence  $\alpha < 2$  (see the Appendix). The classical stability limit for conservative mass transfer ( $D_c = 0$ ) is at  $\alpha = 0$ , while  $\alpha < 0$  describes systems where mass transfer would be dynamically unstable in the absence of nova outbursts.

As can be seen from Fig. 2 the character of  $w(x)$  changes at  $\alpha = 1$  (note that  $w(1) = 1$  in all cases):

- If  $2 > \alpha > 1$  the function  $w(x)$  reaches a maximum at some  $x = x_0$ , and  $w(x) \rightarrow 1$  for  $x \rightarrow \infty$ . We have  $w \leq w(x_0) < 2$  in all cases. For the limiting case  $\alpha = 1$ ,  $w(x)$  is monotonically increasing and approaches the value  $w = 2$  asymptotically. We conclude that for  $\alpha \geq 1$  the mass transfer rate spectrum is always narrow.
- If  $\alpha < 1$ ,  $w(x)$  is monotonically increasing without bound. The slope of  $w(x)$  increases with decreasing  $\alpha$ . We have  $w(x) = x$  for  $\alpha = 0$ . The condition  $w > 10$  can be met in all cases, for any  $x > x_{\text{crit}}$ , but  $x_{\text{crit}}$  is a function of  $\alpha$  (shown in Fig. 3). As  $\alpha$  is in turn a function of mass ratio and adiabatic stellar index, the requirement  $\alpha < 1$  is equivalent to a condition of the form  $q > q_{\text{crit}}$ . A good approximation is

$$q_{\text{crit}} \simeq 0.45 + 0.4 \left( \zeta + \frac{1}{3} \right). \quad (24)$$

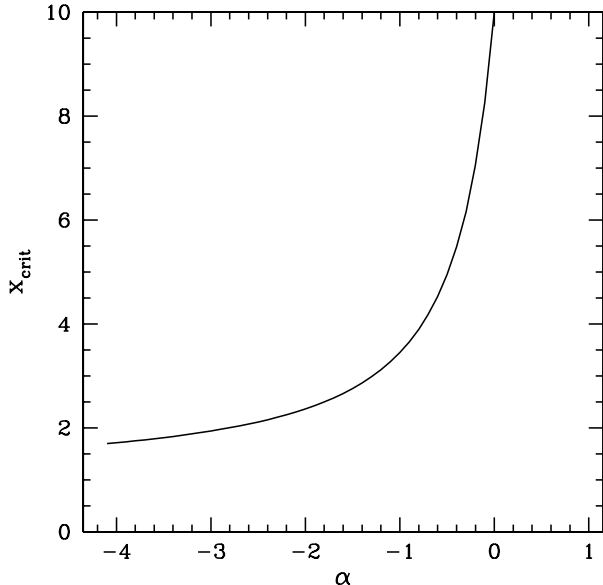


FIG. 3.— The minimal mass accumulation factor  $x_{\text{crit}}(\alpha)$  to obtain  $w(x) > 10$ .

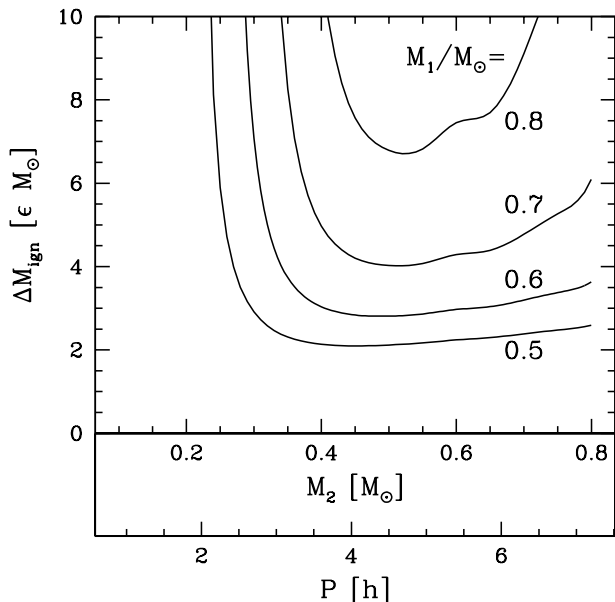


FIG. 4.— Lower limit on the nova trigger mass  $\Delta M_{\text{ign}}$  for nova-induced widths of the mass transfer rate spectrum in excess of a factor 10.  $\Delta M_{\text{ign}}$  is in units of  $\epsilon \simeq 10^{-4} M_{\odot}$  and shown as a function of donor mass  $M_2$  or orbital period  $P/\text{hr} = 9(M_2/M_{\odot})$ , for different white dwarf masses  $M_1$ , as labelled.

The critical conditions  $q > q_{\text{crit}}$ ,  $x > x_{\text{crit}}$  signaling “wide” mass transfer rate distributions becomes more transparent when expressed as constraints on physical system parameters. For a given WD mass the secondary mass  $M_2$  has to be large enough so that the system is not too far from mass transfer instability, and the nova outburst trigger mass has to be larger than a certain lower limit,  $\Delta M_{\text{ign}} > \Delta M_{\text{lim}}$ . Specifically, the former requirement is satisfied when  $q > q_{\text{crit}}$ , where  $q_{\text{crit}}$  is given by equation (24) and is typically within a factor of  $\sim 1.5$  (smaller than)

the value of  $q$  required for mass transfer stability in the absence of nova explosions. Both requirements are summarized in Fig. 4 where we plot  $\Delta M_{\text{lim}}$  (in units of  $\epsilon M_{\odot}$ ) as a function of  $M_2$  for various  $M_1$ . In calculating these limits we assumed that  $\gamma = 1$ , i.e., the mass of the ejected nova envelope is equal to the mass accreted since the last nova outburst (this affects  $D_m$ ) and that the secondary’s adiabatic mass–radius index  $\zeta$  is the same as for a ZAMS star with mass  $M_2$  (shown in Fig. 5). The figure also gives a rough estimate of the orbital period the corresponding CV would have,  $P/\text{hr} \simeq 9(M_2/M_{\odot})$ .

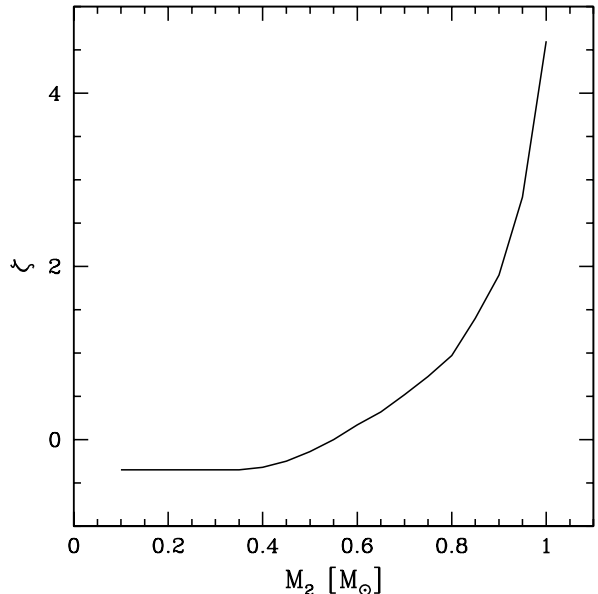


FIG. 5.— The adiabatic stellar mass radius index  $\zeta$  as a function of stellar mass, for Population I ZAMS stars (from Hjellming 1989).

The main conclusions to be drawn from Fig. 4 are:

The nova-induced width of mass transfer spectra is *insignificant* below the CV period gap ( $P \lesssim 2$  hr). These short-period systems are not close enough to instability, i.e., they do not conform to the mass ratio criterion  $q \gtrsim 0.5$ . For the same reason the nova-induced width is negligible whenever the white dwarf is massive ( $M_1 \gtrsim 1 M_{\odot}$ ), whatever the orbital period.

Significant nova-induced widths to the mass transfer rate spectrum can occur above the period gap, for systems with C/O white dwarfs of mass  $0.55 - 0.8 M_{\odot}$  and secondaries with mass close to the stability limit  $M_2 \lesssim 0.7 M_1$ . A necessary requirement is, however, that nova trigger masses are in excess of a few times  $10^{-4} M_{\odot}$ . The actual value depends on the photospheric scale height  $H$  of the donor star, and *increases* with increasing white dwarf mass. It is interesting to note that theoretical outburst calculations unanimously predict that the trigger mass *decreases* with increasing white dwarf mass. Hence we might expect that in a realistic CV population only those C/O white dwarfs with the smallest mass contribute to an effective widening.

Chiefly, significant widths in  $\dot{M}$  can occur above the period gap, but should be least pronounced immediately above the gap and for long  $P$ .

In the next section we demonstrate the analytic findings

in full population synthesis models.

#### 4. POPULATION SYNTHESIS MODELS

In the previous sections, we have shown with an analytic model how the mass transfer rate in a CV evolves with time during the intervals between nova explosions (eq. 14). We then further derived analytic expressions for the corresponding probability density distribution in  $\dot{M}$  (eqs. 16 and 17), and the half width of this distribution (eq. 22). These expressions are straightforward to evaluate for a given binary system in a particular evolutionary state. The behavior of the probability density distribution is a sensitive function of the binary properties, including the mass ratio and the stability ratio (eq. 20); this dependence is illustrated in Figures 2 – 5. In order to compare these results with observational data we would like to know what the width in  $\dot{M}$  is as a function of orbital period for the *ensemble* of CV systems that populate the Galaxy.

In order to explore how broad the range in  $\dot{M}$  would be for an observed collection of CVs with different evolutionary histories and binary parameters, we have carried out a population synthesis study with the effects of nova explosions incorporated. The basic approach to the population synthesis is discussed in detail in Howell, Nelson, & Rappaport (2001, HNR; see also Kolb 1993, and Kolb 1996, 2001 for reviews). We start with a large sample ( $\sim 3 \times 10^6$ ) of primordial binaries whose properties are chosen via Monte Carlo techniques. The primary mass is chosen from an assumed initial mass function (IMF; Miller & Scalo 1979; Eggleton 2001). We adopt a distribution of mass ratios for primordial binaries,  $p(q)$ , which is approximately flat (see, e.g., Duquennoy & Mayor 1991). The initial orbital period,  $P_{\text{orb}}$ , is chosen from a function which is constant in  $\log P_{\text{orb}}$  (see, e.g., Duquennoy & Mayor 1991; Abt & Levy 1985).

The evolution of these systems is followed to see which ones undergo a common envelope phase. In such events, the envelope of the evolved giant primary engulfs the secondary, leading to a spiral-in episode which leaves the secondary in a close orbit with a white dwarf. We adopt the standard approach of assuming that some fraction,  $\alpha_{\text{CE}} \sim 1$ , of the initial orbital binding energy is deposited into the CE as frictional luminosity (see, e.g., Meyer & Meyer-Hofmeister 1979; Sandquist, Taam, & Burkert 2000). Primordial binaries that are too wide will not undergo any significant mass transfer and will not lead to the formation of CV systems – such wide systems are discarded in the present study. Successful pre-cataclysmic variable systems to emerge from the first part of the population synthesis calculations are those which do undergo a common envelope phase and yield a close binary consisting of a white dwarf and low mass ( $\lesssim 1 M_{\odot}$ ) companion.

The second part of the population synthesis considers those white-dwarf main-sequence binaries for which systemic angular momentum losses, or a modest amount of evolution by the normal companion star, can initiate Roche-lobe contact within a Hubble time. At the start of mass transfer from the original secondary to the white dwarf the mass transfer may be driven by systemic angular momentum losses, or if the secondary has a mass which is too large, the transfer may proceed on either a thermal or dynamical timescale. We do not consider either of these

latter two cases, although the former most likely leads to a “cousin” of CVs, the supersoft X-ray sources (see, e.g., Kahabka & van den Heuvel 1997). Tests for stability at the onset of mass transfer and all other phases of the CV evolution are done in the binary evolution code by requiring that  $D$  as defined in equation (8) is always positive. The binary evolution code is the same as that used by HNR which, in turn, is a descendant of the code developed by RVJ, and is based on a bipolytropic stellar structure. Each of the CV systems is evolved in detail through the mass-transfer phase (CV phase) until the donor star has been reduced to a negligible mass (typically  $0.03 M_{\odot}$ ). The expression for magnetic braking, which is the principal driver of mass transfer for systems above the period gap, is taken from RVJ and Verbunt & Zwaan (1981) and adopts values for RVJ’s parameters of  $\gamma_{\text{RVJ}} = 3$  and  $f = 1.0$ . In a typical population synthesis run, some  $\sim 2 \times 10^4$  such binaries are evolved through the CV phase.

We have modified the treatment of mass transfer in the bipolytrope code so that we can explicitly follow the movement of the Roche lobe through the atmosphere of the donor star as the system evolves between nova explosions. A few illustrative binary evolution runs were made with this modified code (these are not used or presented in this paper). However, this type of explicit calculation requires very short timesteps (sometimes as short as years), and is therefore very computationally intensive for use in a population synthesis study. Fortunately, the binary system and donor star properties do not evolve significantly during a single interval between nova explosions, and therefore much of the analytic formalism developed in this paper can be simply carried over to the population synthesis calculations. In fact Schenker et al. (1998) showed explicitly that CV evolution with the appropriate steady mass-loss rate approximates, to a high degree, the average evolution of a CV with discrete nova mass loss events. Thus, in the population synthesis study we utilize a steady mass loss rate wherein the ejected matter in nova explosions carries away the specific angular momentum of the white dwarf.

For each time step in the evolution of a particular CV we store the amount of time the system spends within a given range of  $\dot{M}$  and  $P_{\text{orb}}$ . However, for each time step, in addition to recording the actual computed value of  $\dot{M}$  which represents the case of continuous mass loss, we utilize equations (14) and (17) to tell us how  $\dot{M}$  is distributed in the nova-evolution case. We take from the binary evolution code instantaneous parameters such as the stellar masses, atmospheric scale height, average time to accrete an ignition mass, adiabatic stellar index, and so forth, i.e., all the parameters necessary to evaluate equations (14) and (17).

The results are shown first in the  $\dot{M} - P_{\text{orb}}$  plane, color coded according to the logarithm of the probability of finding a system in a particular part of this parameter space. In Figure 6a the results are shown for the case of a steady mass loss instead of the more appropriate discrete nova mass-loss events (see also HNR). Note that for systems above the period gap the half width of the distribution in  $\dot{M}$  at any given value of  $P_{\text{orb}}$  is no greater than a factor of  $\sim 2$ . In Fig. 6b the same results are shown for the case of discrete nova events, where the ignition mass is taken to

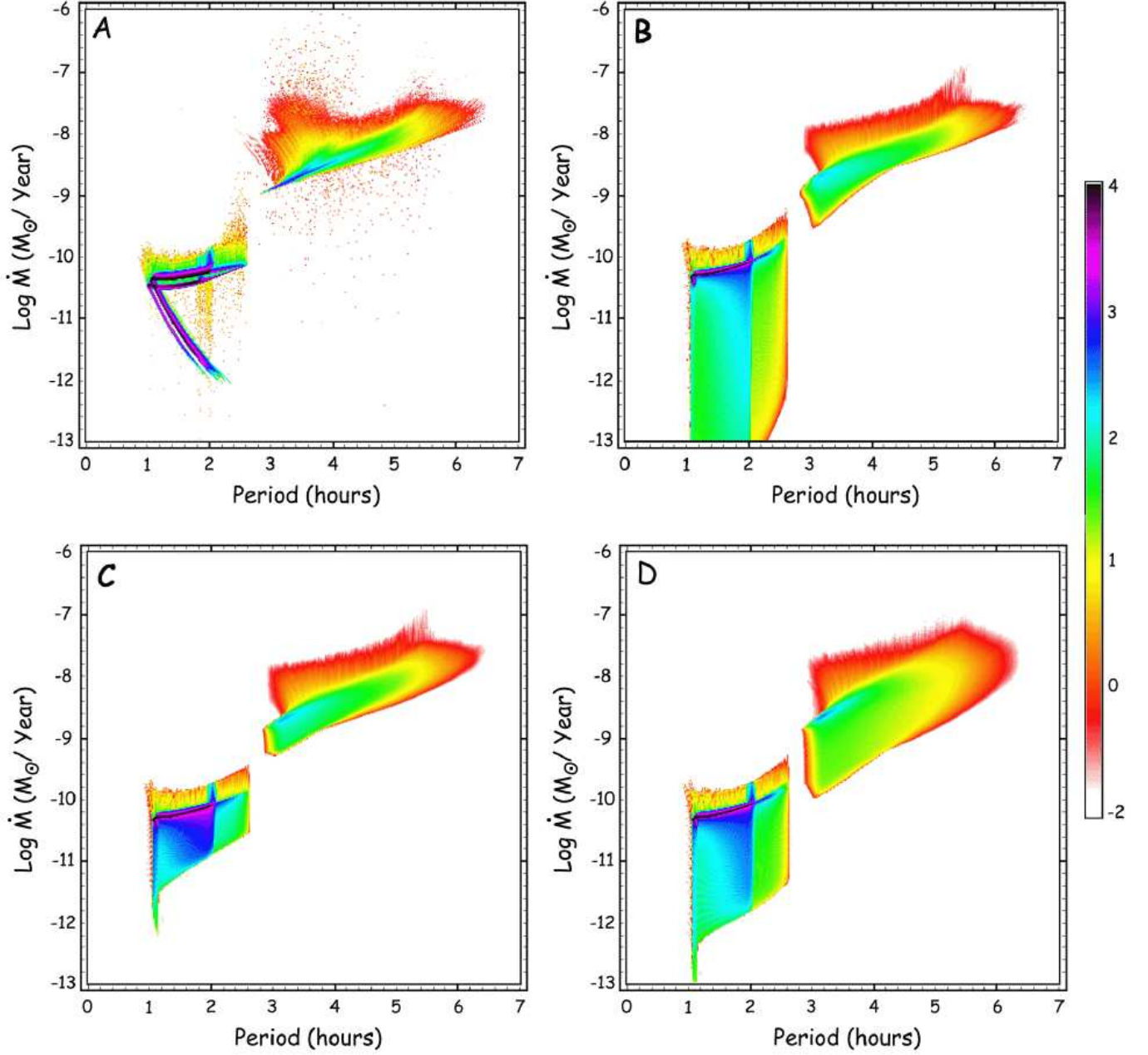


FIG. 6.— Probability density distribution (PDF) of a CV population in the orbital period - mass transfer rate plane. The color-code refers to  $\log(\text{PDF})$ . See text for details. *Panel A:* Mean evolution, no novae. *Panel B:* Effect of novae taken into account, trigger masses given by eq. 25. *Panel C:* Effect of novae taken into account, trigger mass  $1 \times 10^{-4} M_\odot = \text{const.}$  *Panel D:* Effect of novae taken into account, trigger mass  $3 \times 10^{-4} M_\odot = \text{const.}$



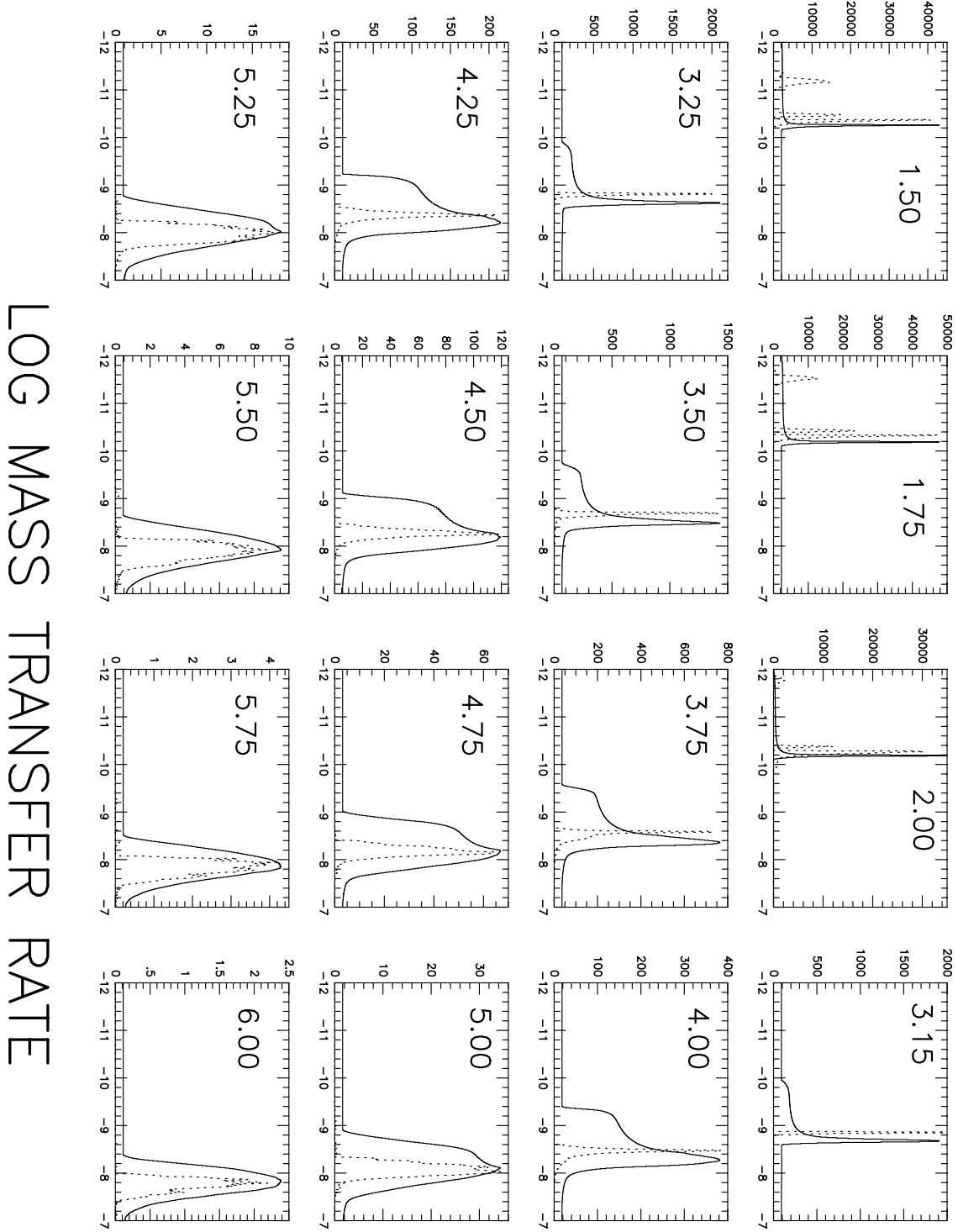


FIG. 7.— Slices in orbital period of the PDFs shown in Fig. 6, on a linear scale. Solid curves: trigger mass  $3 \times 10^{-4} M_{\odot}$  (Fig. 6d). Dashed: no nova case (Fig. 6a). Each panel is labelled with the corresponding orbital period in hrs.

be

$$\Delta M_{\text{ign}} \simeq 4.4 \times 10^{-4} M_{\odot} \times \left( \frac{R_1}{10^9 \text{cm}} \right)^4 \left( \frac{M_1}{M_{\odot}} \right) \left( \frac{\dot{M}}{10^{-9} M_{\odot} \text{yr}^{-1}} \right)^{-1/3} \quad (25)$$

( $R_1$  is the white dwarf radius). This is an approximate analytic fit (cf. Kolb 1995) to results from fully time-dependent thermonuclear runaway (TNR) calculations for cold (old) white dwarfs by Prialnik & Kovetz (1995), which we use for illustrative purposes only. For the WD radius we used the approximation by Nauenberg (1972)

$$\frac{R_1}{R_{\odot}} = 0.0112 \left\{ \left( \frac{M_1}{1.44 M_{\odot}} \right)^{-2/3} - \left( \frac{M_1}{1.44 M_{\odot}} \right)^{2/3} \right\}^{1/2} \quad (26)$$

We also tested other expressions that fit TNR calculations reported in Nomoto 1982, and semi-analytic solutions to the thermal equilibrium behavior of H-rich shells given by Fujimoto (1982). The population synthesis results are quite similar in all cases. In the results leading to Fig. 6b all CVs with He white dwarf accretors have been eliminated. This is due to the uncertainties in our understanding of the stability and properties of the nuclear burning on the surfaces of such low-mass white dwarfs. Note that for the remaining systems, most of which would have CO white dwarfs, the width of the  $\dot{M}$  distribution at a given  $P_{\text{orb}}$  is somewhat broader than in the case of CV evolution without novae (e.g., Fig. 6a). For systems above the period gap the full width at 50 percent probability of the  $\dot{M}$  distribution is about a factor of 3, but is still not nearly broad enough to explain the observational data on CVs. By contrast, for systems below the period gap, the width looks quite broad due to the logarithmic color coding; however, a more quantitative look (see also Fig. 7) will show that most systems would have values of  $\dot{M}$  closely bunched around the values found in the no-nova case. The long colored tail which appears toward lower  $\dot{M}$  has quite small probability densities (see e.g. Figure 1), consistent with the findings of Section 3.

Finally, in Fig. 6c and Fig. 6d we show the results for the somewhat *ad hoc* assumption that all novae burn and eject  $1 \times 10^{-4} M_{\odot}$  or  $3 \times 10^{-4} M_{\odot}$  of matter. Fig. 6c, for  $dM_{\text{ign}} = 1 \times 10^{-4} M_{\odot}$ , shows a rather uniform width in  $\dot{M}$  (above the period gap) of about a factor of 3, which is comparable with that for the case where  $dM_{\text{ign}}$  is calculated from equation (25) (see Fig. 6b). In contrast, the distributions in Fig. 6d, which were computed for the case where  $dM_{\text{ign}} = 3 \times 10^{-4} M_{\odot}$ , show a width in  $\dot{M}$  that is nearly a factor of 10, in reasonable agreement with the observations.

The color-coded images provide a qualitative overview of the evolutionary properties expected for CVs in the  $\dot{M} - P_{\text{orb}}$  plane. However, for a more quantitative view we take slices in orbital period and plot ordinary linear histograms of the distribution in  $\dot{M}$  for each of 16 intervals of  $P_{\text{orb}}$ . The results corresponding to the color image of Fig. 6d are shown in Fig. 7 as solid curves. The dashed curves (narrower distributions) are for the no-nova cases and are shown for purpose of comparison. In each panel, the interval in  $P_{\text{orb}}$  is typically 1/4 hr wide, and centered

on the value indicated in that panel. A perusal of this figure confirms the description of the width in  $\dot{M}$  for various regions of  $P_{\text{orb}}$  as discussed in connection with the color figures in the  $P_{\text{orb}} - \dot{M}$  plane, and the analytic expressions for the mass transfer rate spectrum in section 3.3.

We note that for donors with mass  $\gtrsim 0.6 M_{\odot}$  the bipolytrope models underestimate the adiabatic stellar index. This might cause a slight overestimate of the width of the mass transfer rate spectrum at periods longer than about 5 hrs.

## 5. DISCUSSION

We have investigated the width of the distribution of mass transfer rates for CVs with similar orbital period, induced by nova outbursts, as a function of orbital period. We used a semi-analytical model that describes the time evolution of the mass transfer rate between outbursts to probe the parameter space. A detailed population synthesis model demonstrates the overall effect on a population of CVs with standard assumptions about formation and evolution.

CVs where mass transfer is close to instability or unstable, in the absence of nova outbursts, but stabilized through outbursts, contribute most to an effective widening of the  $\dot{M}$  distribution. Hence the effect is most pronounced where this instability occurs, i.e., in systems with large mass ratio  $M_2/M_1$ . For this reason the effect is insignificant below the period gap (despite possibly large ratios of maximum to minimum values of  $\dot{M}$  after and prior to nova explosions), and at long orbital periods where all CVs are dynamically stable. In the intermediate period regime, chiefly between 3 and 6 hrs, a surprisingly large fraction of CVs are close to the optimum parameter range that maximizes the impact of novae on the spread of  $\dot{M}$ . The main contribution is from systems with white dwarf masses less than  $0.8 M_{\odot}$ .

We find that the spread of mass transfer rates is significant, i.e., covering an order of magnitude, only if the mass accreted between two outbursts exceeds a few times  $10^{-4} M_{\odot}$ . This critical value increases with increasing white dwarf mass, and is inversely proportional to the relative scale height  $H/R$  of the donor star's photosphere.

Our goal was to determine the maximum effect of nova outbursts on the spread of  $\dot{M}$  values. Therefore we assumed in our analysis that there are no frictional orbital angular momentum losses due to the orbital motion of the secondary inside the expanding nova envelope. In that case the mass transfer rate always decreases as a result of an outburst. If there is dynamical friction, the decrease of  $\dot{M}$  becomes smaller with increasing friction, and eventually turns into an increase (see, e.g., Schenker et al. 1998). A similarly large amplitude change in  $\dot{M}$  as in the absence of friction, but in the opposite direction, requires an implausibly strong dynamical friction.

We assumed further that the mass of the ejected nova envelope is equal to the mass the white dwarf accretes between two outbursts (i.e.,  $\gamma = 1$ ). The effect of changing  $\gamma$  is mainly felt through the stability of the systems. A larger  $\gamma$  decreases  $\zeta_m$ , see equation (A10), and hence widens the parameter space available to systems that are dynamically unstable in the absence of nova outbursts but stable with

outbursts. Hence any  $\gamma > 1$  increases the effect of novae on the spread of  $\dot{M}$ , while any  $\gamma < 1$  decreases the effect, compared to the case we have investigated in detail. If  $\gamma = 2$  (i.e., the white dwarf ejects twice as much mass as it has accreted) the limiting accreted mass required to cause a half width of an order of magnitude for CVs with a  $0.6 M_\odot$  WD decreases from  $3.0 \times 10^{-4} M_\odot$  to  $1.5 \times 10^{-4} M_\odot$ . At the same time the curves in Fig. 4 extend to somewhat smaller values of  $M_2$ . On the other hand, if  $\gamma = 0.8$  (i.e., the white dwarf retains 20% of the mass accreted previously) the limiting mass becomes  $3.5 \times 10^{-4} M_\odot$ . The curves in Fig. 4 move up, those for higher  $M_1$  more so than those for lower  $M_1$ . Systems with  $M_1 = 0.5 M_\odot$  and  $M_2 \gtrsim 0.5 M_\odot$  are dynamically unstable even in the presence of nova outbursts.

Another effect that could reduce the impact of nova outbursts on the mass transfer rate spectrum is wind losses from the disk prior to outburst, so that the white dwarf accretes less mass than is actually transferred via Roche lobe overflow. If this mass carries away the specific orbital angular momentum of the white dwarf the effect is that the Roche lobe index describing the evolution between two outbursts is no longer the conservative one, but a smaller one, given by equation (A10), with  $\gamma$  now referring to the fraction of transferred mass that is lost in the wind. The net effect is to stabilize the systems, and hence to reduce the parameter space available to nova-stabilized systems.

Finally, any weighting in favor of bright systems will make the maximum of the mass transfer rate spectra seen in Fig. 7 more pronounced, i.e., the distribution of  $\dot{M}$  will be more skewed. The distributions will therefore appear narrower.

Our results are largely independent of the assumed functional form of the magnetic braking law. The differential effect of nova outbursts on the width of the mass transfer rate spectrum is the same for any orbital braking law. This is significant for the relative distribution of dwarf novae and novalikes as a function of orbital period. If the critical rate for stable disk accretion separates these two classes, then a suitably chosen orbital braking strength, combined with the nova-induced  $\dot{M}$  spread, can reproduce the observed relative distribution.

A particularly striking detail of the population synthesis simulations is the effect on the mass transfer rate spectrum at periods immediately above the gap (Fig. 7). The unwidened distribution is narrow and centered on  $\dot{M} \simeq 1.5 \times 10^{-9} M_\odot \text{yr}^{-1}$ . In the standard model, the width of the period gap essentially fixes this value, and provides a calibration for the magnetic braking strength (see, e.g. Kolb 1996). As noted already by Shafter (1992), this rate is lower than the critical rate for disk stability, hence suggesting that just above the gap most CVs should be dwarf novae. The exact opposite is observed (e.g. Ritter & Kolb 1998). Significantly, the nova-widened  $\dot{M}$  distribution has a pronounced maximum above the secular mean, at  $\dot{M} \simeq 2.5 \times 10^{-9} M_\odot \text{yr}^{-1}$  (see panel for  $P = 3.15$  hrs in Fig. 7), thus allowing a fraction of systems to appear as novalikes. Note, however, that the nova widening does not affect the mean value of the  $\dot{M}$  distribution at any given orbital period. Hence in the nova-widened distributions shown in Fig. 7 there would still be more dwarf novae than novalikes immediately above the period gap. This is

different if there is an observational selection effect in favor of brighter systems. If the selection is strong enough dwarf novae that are present in the intrinsic population could be effectively suppressed in the observed sample.

A comment on “hibernation” is in order. In the ballistic ejection cases considered here the post nova transfer rate can indeed be much smaller — by one or two orders of magnitude — than the secular mean rate (see, e.g., Fig. 1). Generally, after an outburst the systems evolve back close to the secular mean within a time  $f_n t_{\text{rec}}$  which is a fraction  $f_n < 1$  of the nova recurrence time  $t_{\text{rec}}$ . At periods where the nova-induced spread of transfer rates is negligible, e.g., below the CV period gap,  $f_n \lesssim 0.1$ , while for systems close to dynamical instability  $f_n \simeq 0.5$  (see, e.g., Fig 1). In other words, the majority of CVs spend a significant fraction of their time close to the secular mean. This is the converse of the original hibernation model hypothesis  $f_n \sim 1$ . As recurrence times are generally very long,  $10^4$  yrs or longer, this is consistent with observations of apparently very faint post nova systems for the few observed historical novae which obviously had at most a few centuries to recover from the outburst. A similar conclusion was reached by Iben, Fujimoto & MacDonald (1995; their Appendix B).

Our findings rely on the assumption that the majority of CV secondaries are unevolved, i.e., main-sequence stars (not necessarily in thermal equilibrium) where core hydrogen depletion is not yet very advanced. This is consistent with the standard model of CV formation, as employed in our population synthesis calculations. There is evidence, however, that a significant fraction of CVs do have a somewhat evolved donor star (Baraffe & Kolb 2000; see also Kolb 2001). This should be followed up by future studies.

We note that Spruit & Taam (2001) have discussed the fluctuation of  $\dot{M}$  in the context of a hypothetical circumbinary disk, but had difficulties finding a convincing model that would at the same time preserve the orbital period gap of CVs.

Irradiation (Ritter, Zhang & Kolb 2000, and references therein) has been considered as an effect that superposes mass transfer cycles, on the thermal time of the donor star, onto the secular mean without changing the mean. Without additional driving mechanisms, such as the coupling to a consequential angular momentum loss (e.g. McCormick & Frank 1998) all indications suggest that irradiation-driven cycles disappear for systems with donor mass  $\lesssim 0.7 M_\odot$ .

We conclude that nova-induced variations of the mass transfer rate may account for the observed spread of  $\dot{M}$  above the period gap, but only if the trigger masses on intermediate-mass C/O white dwarfs are in excess of  $\sim 2 \times 10^{-4} M_\odot$ . CVs with the highest transfer rates should be close to mass transfer instability, i.e., should have a fairly large mass ratio. This constitutes an observational test of the nova-induced spread of CV transfer rates.

We are grateful to Lorne Nelson, Andrew King and Hans Ritter for useful discussions. We thank Mike Shara and Goce Zojcheski for their participation in an earlier phase of this research. Comments by the anonymous referee helped to improve the presentation of the paper. Bart Willems

spotted an inconsistent definition of  $\beta_2$ . This research was supported in part by PPARC (UK), and by NASA under ATP grants GSFC-070 and NAG5-8500 (to SBH),

and NAG5-7479 and NAG5-4057 (to SAR). UK thanks the Aspen Center for Physics (where this work has been completed) for hospitality and support.

## APPENDIX

### ANALYTICAL MODEL: FURTHER DETAILS

This appendix provides details and derivations for the model developed in Section 3.

#### *The Roche-lobe index*

The stationary mass transfer rate (11) depends on the Roche lobe index  $\zeta_L$ . We obtain  $\zeta_L$  by comparing the definition (5) with the time derivative of

$$J = M_1 M_2 \sqrt{\frac{G a}{M_b}} \quad (\text{A1})$$

( $a$  is the orbital separation,  $M_b = M_1 + M_2$  the total binary mass), and by noting that  $R_L/a$  is a function of mass ratio  $q = M_2/M_1$  only. The time derivative of the left hand side of (A1) is the sum  $\dot{J}_{\text{sys}} + \dot{J}_{\text{ej}}$  of systemic losses and losses due to mass that is ejected from the system. We parametrize the latter by

$$\dot{J}_{\text{ej}} = \nu \frac{J}{M_b} \dot{M}_b, \quad (\text{A2})$$

so that  $\nu$  measures the specific angular momentum of the mass lost from the binary, in units of the mean specific angular momentum of the orbit. We further assume that the mass lost from the system is a fraction  $\gamma > 0$  of the transferred mass,

$$\dot{M}_b = \gamma \dot{M}_2 \quad \text{or} \quad \dot{M}_1 = (\gamma - 1) \dot{M}_2. \quad (\text{A3})$$

This is consistent with the definition of  $\gamma$  in (12) if (A3) is understood as the net effect over one nova cycle.

Using the notation

$$\beta_2 = \frac{q}{R_L/a} \frac{dR_L/a}{dq} \quad (\text{A4})$$

this finally gives

$$\zeta_L = \gamma \left\{ (2\nu + 1) \frac{M_2}{M_b} + (-\beta_2 - 2) \frac{M_2}{M_1} \right\} + \zeta_c, \quad (\text{A5})$$

with  $\zeta_c$ , the Roche lobe index for conservative mass transfer ( $\gamma = 0$ ), given by

$$\zeta_c = 2 \frac{M_2 - M_1}{M_1} + \frac{M_b}{M_1} \beta_2. \quad (\text{A6})$$

If  $q \lesssim 1$  we have  $R_L/a \simeq 0.46(M_2/M)^{1/3}$  (Paczynski 1971), hence

$$\beta_2 \simeq \frac{1}{3} \frac{M_1}{M_b} \quad (\text{A7})$$

so that

$$\zeta_L \simeq \gamma \left\{ 2\nu \frac{M_2}{M_b} + \frac{2}{3} \frac{M_2}{M_b} - 2 \frac{M_2}{M_1} \right\} + \zeta_c, \quad (\text{A8})$$

and  $\zeta_c$  simplifies to the standard expression

$$\zeta_c \simeq 2 \frac{M_2}{M_1} - \frac{5}{3}. \quad (\text{A9})$$

#### *Mean evolution*

If the nova ejecta carry the specific orbital angular momentum of the WD we have  $\nu = M_2/M_1$ , and (A8) simplifies to

$$\zeta_m \simeq -\gamma \frac{4}{3} \frac{M_2}{M_b} + \zeta_c. \quad (\text{A10})$$

The corresponding long-term mean mass transfer rate introduced by (15), the “isotropic wind-average”, is

$$\dot{M}_m = \frac{M_2/t_{\text{ev}}}{D_m} \quad (\text{A11})$$

with  $D_m = \zeta - \zeta_m$ , cf. (11). The equivalent expression with  $D_c = \zeta - \zeta_c$ ,

$$\dot{M}_c = \frac{M_2/t_{\text{ev}}}{D_c} \quad (\text{A12})$$

represents the conservative stationary rate the system would adopt in the absence of nova outbursts if  $D_c > 0$ . If the conservative evolution is dynamically unstable, i.e.,  $D_c < 0$ , the quantity  $\dot{M}_c$  as defined in (A12) is still the relevant quantity to use in the expression for the time evolution of  $\dot{M}$ , equation (14).

In the derivation presented here we assume that the thermal relaxation term  $(\partial \ln R / \partial t)_{\text{th}}$  which builds up in the donor star experiencing a discontinuous mass loss history due to nova outbursts is the same as in the time-averaged, continuous evolution. In other words,  $t_{\text{ev}}$  in (A11) is the same as in (14). This has been confirmed by detailed integrations of the secular evolution using full stellar models.

### Outburst amplitude

The outburst amplitude ratio  $\dot{M}_f/\dot{M}_0$  of the mass transfer rate ( $\dot{M}_f$  is  $\dot{M}$  at  $t = t_{\text{rec}}$ ) can be calculated from the ejected envelope mass. From (2) we have

$$\frac{\dot{M}_f}{\dot{M}_0} = \frac{\dot{M}(\text{pre-nova})}{\dot{M}(\text{post-nova})} = \exp \left\{ \frac{1}{\epsilon} \left( \frac{\Delta R_L}{R_L} \right)_{\text{out}} \right\}, \quad (\text{A13})$$

where the index “out” refers to the nova outburst. Using (5) the total change  $(\Delta R_L/R_L)_{\text{total}}$  of the Roche lobe radius over one outburst cycle (outburst, followed by conservative evolution until the next outburst) can be written as

$$\left( \frac{\Delta R_L}{R_L} \right)_{\text{total}} = \left( \frac{\Delta R_L}{R_L} \right)_{\text{out}} + \left( \frac{\Delta R_L}{R_L} \right)_{\text{inter}} = \zeta_m \frac{\Delta M_2}{M_2} + \left( \frac{\Delta J_{\text{sys}}}{J} \right)_{\text{inter}}, \quad (\text{A14})$$

while

$$\left( \frac{\Delta R_L}{R_L} \right)_{\text{inter}} = \zeta_c \frac{\Delta M_2}{M_2} + \left( \frac{\Delta J_{\text{sys}}}{J} \right)_{\text{inter}}. \quad (\text{A15})$$

Here “inter” refers to the evolution between two outbursts, and  $-\Delta M_2 = \Delta M_{\text{ign}} > 0$  is the mass transferred in this phase. Hence we have

$$\left( \frac{\Delta R_L}{R_L} \right)_{\text{out}} = (\zeta_m - \zeta_c) \frac{\Delta M_2}{M_2} = (D_c - D_m) \frac{\Delta M_2}{M_2}. \quad (\text{A16})$$

Using (A16) in (A13) we find

$$\frac{\dot{M}_f}{\dot{M}_0} = \exp \left\{ \frac{1}{\epsilon} (D_m - D_c) \frac{\Delta M_{\text{ign}}}{M_2} \right\} \quad (\text{A17})$$

With (A10) for  $\zeta_m$  this simplifies to equation (13) given in Section 3.2.

### The mass transfer rate spectrum

The integrated form of the mass transfer spectrum (17) is

$$t(\dot{M}) = \epsilon t_{\text{ev}} \ln \left\{ \frac{\dot{M}(\dot{M}_c - \dot{M}_0)}{\dot{M}_0(\dot{M}_c - \dot{M})} \right\} \quad (\text{A18})$$

cf. Equation (14).

To calculate either (A18) or (17) for systems with specified masses and secular mean rate we need to find  $\dot{M}_0$ . This can be obtained as follows. From (14) at  $t = t_{\text{rec}}$  we have

$$\frac{\dot{M}_0}{\dot{M}_c} = \frac{\dot{M}_0/\dot{M}_f - \exp\{-t_{\text{rec}}/\epsilon t_{\text{ev}}\}}{1 - \exp\{-t_{\text{rec}}/\epsilon t_{\text{ev}}\}}. \quad (\text{A19})$$

Using (A17) to replace  $\dot{M}_0/\dot{M}_f$  and noting that

$$\frac{t_{\text{rec}}}{\epsilon t_{\text{ev}}} = \frac{\Delta M_{\text{ign}}/\dot{M}_m}{\epsilon t_{\text{ev}}} = \frac{D_m}{\epsilon} \frac{\Delta M_{\text{ign}}}{M_2}, \quad (\text{A20})$$

(cf. (15) and (A11)) we finally find

$$\frac{\dot{M}_0}{\dot{M}_c} = \frac{\exp\{D_c \Delta M_{\text{ign}}/\epsilon M_2\} - 1}{\exp\{D_m \Delta M_{\text{ign}}/\epsilon M_2\} - 1}. \quad (\text{A21})$$

### REFERENCES

- Abt, H.A., & Levy, S.G. 1985, ApJS, 59, 229  
 Baraffe, I., & Kolb, U. 2000, MNRAS, 318, 354  
 Baptista, R. 2000, in Astro-Tomography Workshop, H. Boffin, D. Steeghs, Lecture Notes in Physics, Springer: Berlin, in press (astro-ph/0009472)  
 Cannizzo, J.K., Shafter, A.W., & Wheeler, J.C. 1988, ApJ, 333, 227  
 Duquennoy, A. & Mayor, M. 1991, A&A, 248, 485  
 Eggleton, P. 2001, Evolutionary Processes in Binary and Multiple Stars (Cambridge: Cambridge Univ. Press), in preparation  
 Frank, J., King, A. & Raine, D., 1992, Accretion Power in Astrophysics, Cambridge University Press, Chps, 4-6.  
 Fujimoto, M.Y. 1982, ApJ, 257, 767  
 Hameury, J.M., King, A.R., Lasota, J.P., & Ritter, H. 1988, MNRAS, 231, 535  
 Hjellming, M.S. 1989, PhD thesis, University of Illinois, Urbana-Champaign  
 Horne, K. 1985,, MNRAS, 213, 129  
 Howell, S., Nelson, L.A., & Rappaport, S.A. 2001, ApJ, 1 April issue (HNR)  
 Iben, I., Fujimoto, M.Y., & MacDonald, J. 1992, ApJ, 388, 521  
 Kahabka, P., & van den Heuvel, E. P. J. 1997, ARA&A, 35, 69  
 King, A.R. 1988, QJRAS, 29, 1  
 King, A.R., & Kolb, U. 1995, ApJ, 439, 330  
 Kolb, U. 1993, A&A, 271, 149  
 Kolb, U. 1995, in Cataclysmic Variables, A. Bianchini, M. Della Valle, and M. Orio, Kluwer: Dordrecht, Astrophysics and Space Science Library, 205, 511  
 Kolb, U. 1996, in Cataclysmic Variables and Related Objects, A. Evans and J.H. Wood, Kluwer: Dordrecht, 433  
 Kolb, U. 2001, in The influence of binaries on stellar population studies, D. Vanbeveren, Kluwer: Dordrecht, in press  
 Kolb, U., & Ritter, H. 1990, A&A, 236, 385  
 Livio, M., & Shara, M.M. 1987, ApJ, 319, 819  
 Livio, M., Govarie, A., & Ritter, H. 1991, A&A, 246, 84

- MacDonald, J. 1986, *ApJ*, 305, 251  
 McCormick, P., & Frank, J. 1998, *ApJ*, 500, 923  
 Meyer, F., & Meyer-Hofmeister, E. 1979, *A&A*, 78, 167  
 Meyer, F., & Meyer-Hofmeister, E. 1981, *A&A*, 104, L10  
 Miller, G.E., & Scalo, J.M. 1979, *ApJS*, 41, 513  
 Nauenberg, M. 1972, *ApJ*, 175, 417  
 Nomoto, K., *ApJ*, 253, 798  
 Paczyński, B. 1971, *ARA&A*, 9, 183  
 Patterson, J. 1984, *ApJS*, 54, 443  
 Patterson, J., & Raymond, J., 1985a, *ApJ*, 292, 535.  
 Patterson, J., & Raymond, J., 1985b, *ApJ*, 292, 550.  
 Prialnik, D. & Shara, M. 1986, *ApJ*, 311, 172  
 Prialnik, D. & Kovetz A. 1995, *ApJ*, 445, 789  
 Rappaport, S., Joss, P.C., & Webbink, R. 1982, *ApJ*, 254, 616 (RJW)  
 Rappaport S., Verbunt F., & Joss, P.C. 1983, *ApJ*, 275, 713 (RVJ)  
 Ritter, H. 1988, *A&A*, 202, 93  
 Ritter, H. 1996, in *Evolutionary Processes in Binary Stars*,  
 R.A.M.J. Wijers, M.B. Davies and C. Tout, Kluwer, Dordrecht,  
 223a  
 Ritter, H., Kolb, U. 1998, *A&AS*, 129, 83  
 Ritter, H., Zhang, Z., Kolb U. 2000, *A&A*, 360, 969  
 Robinson, E.L., Wood, J.H., Wade, R.A. 1999, *ApJ*, 514, 952  
 Sandquist, E., Taam, R., & Burkert, A. 2000, *ApJ*, 533, 984  
 Shara, M., Livio, M., & Moffat, A.F.J., & Orio, M. 1986, *ApJ*, 311,  
 163  
 Schenker, K, Kolb, U., & Ritter, H. 1998, *MNRAS*, 297, 633  
 Shafter, A.W. 1992, *ApJ*, 394, 268  
 Smak, J., 1989, *Acta Astr.*, 39, 317.  
 Smak, J., 1994, *Acta Astr.*, 44, 45.  
 Sproats, L.N., Howell, S.B., & Mason, K.O. 1996, *MNRAS*, 282, 1211  
 Spruit, H.C., & Taam, R.E. 2001, *ApJ*, 548, 900  
 Starrfield, S. 1999, *Physics Reports*, 311, 371  
 Stehle, R., Ritter, H., & Kolb, U. 1996, *MNRAS*, 279, 581  
 Tytenda, R., 1981, *Acta Astr.*, 31, 127.  
 Verbunt, F., & Zwaan, C. 1981, *A&A*, 100, L7  
 Warner, B. 1987, *MNRAS*, 227, 23  
 Warner, B. 1995, *Cataclysmic Variables*, Cambridge Astrophysics  
 Series 28, Cambridge: CUP, Chps 2,9  
 Webbink, R.F. 1985, in *Interacting Binary Stars*, J.E. Pringle and  
 R.A. Wade, CUP: Cambridge, 39

This figure "f6.gif" is available in "gif" format from:

<http://arXiv.org/ps/astro-ph/0108322v1>